

LETTERS

Earth's transmission spectrum from lunar eclipse observations

Enric Pallé¹, María Rosa Zapatero Osorio¹, Rafael Barrena¹, Pilar Montañés-Rodríguez¹ & Eduardo L. Martín^{1,2}

Of the 342 planets so far discovered¹ orbiting other stars, 58 'transit' the stellar disk, meaning that they can be detected through a periodic decrease in the flux of starlight². The light from the star passes through the atmosphere of the planet, and in a few cases the basic atmospheric composition of the planet can be estimated^{3–5}. As we get closer to finding analogues of Earth^{6–8}, an important consideration for the characterization of extrasolar planetary atmospheres is what the transmission spectrum of our planet looks like. Here we report the optical and near-infrared transmission spectrum of the Earth, obtained during a lunar eclipse. Some biologically relevant atmospheric features that are weak in the reflection spectrum⁹ (such as ozone, molecular oxygen, water, carbon dioxide and methane) are much stronger in the transmission spectrum, and indeed stronger than predicted by modelling^{10,11}. We also find the 'fingerprints' of the Earth's ionosphere and of the major atmospheric constituent, molecular nitrogen (N₂), which are missing in the reflection spectrum.

The characterization of spectral features in our planet's transmission spectrum can be achieved through observations of the light reflected from the Moon towards the Earth during a lunar eclipse, which resembles the observing geometry during a planetary transit. At that time, the reflected sunlight from the lunar surface within the Earth's umbra will be entirely dominated by the fraction of sunlight that is transmitted through an atmospheric ring located along the Earth's day–night terminator (Supplementary Fig. 1). Observations of the lunar eclipse on 16 August 2008 have allowed us to characterize the Earth's spectrum as if it were observed from an astronomical distance during a transit in front of the Sun. Except for some early attempts^{12,13} with photographic plates, spectroscopic lunar eclipse observations in visible or near-infrared wavelengths have not previously been undertaken.

The Earth's transmission spectrum can be calculated from the brightness ratio of the light reflected by the lunar surface when in the umbra, in the penumbra and out of the eclipse (Supplementary Information). The resulting transmission spectrum is shown in Fig. 1a, where simultaneous optical and near-infrared observations with the William Herschel and Nordic Optical Telescopes are inter-calibrated to provide continuous wavelength coverage from 0.36 to 2.40 μm . It is known that the Earth's optical and near-infrared transmission spectrum is red¹⁴—that is, more solar flux successfully passes through the atmosphere at longer wavelengths, as can be inferred from simple naked-eye observations of a lunar eclipse, or of a sunset/sunrise. The rising nature of the transmission spectrum continuum towards longer wavelengths (possibly the most remarkable feature of the data shown in Fig. 1a) is caused by the Rayleigh scattering of air, which, in addition to the ozone Chappuis band absorption between 0.375 and 0.650 μm , is rather efficient in scavenging short wavelength radiation through a long atmospheric path.

During a transit, the starlight that passes through the planet's atmosphere travels through a much larger atmospheric path than the starlight that is directly reflected by the planet. This causes the reflection and transmission spectra to be different (see Fig. 1b). In transmission, the Earth is brighter in the near-infrared range, particularly at 2.2 μm .

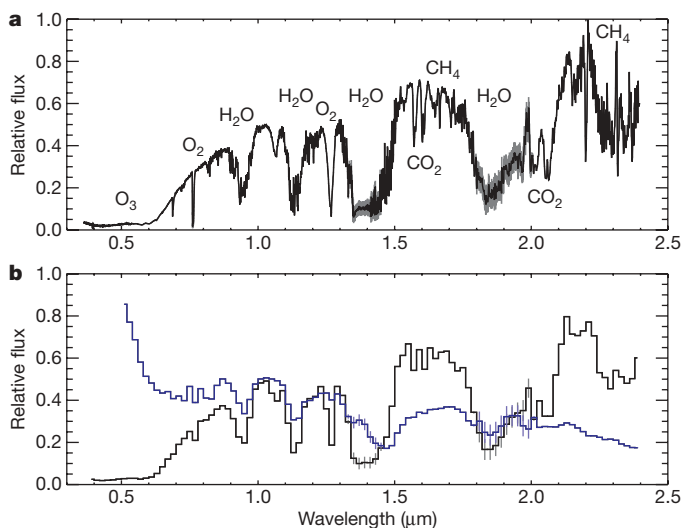


Figure 1 | Earth's visible and near-infrared transmission and reflection spectra. The Earth's transmission spectrum is a proxy for Earth observations during a primary transit as seen beyond the Solar System, while the reflection spectrum is a proxy for the observations of Earth as an exoplanet by direct observation after removal of the Sun's spectral features. **a**, The transmission spectrum, with some of the major atmospheric constituents marked. The spectrum has a resolution of 0.00068 μm in the optical (resolving power, $R \approx 960$) and 0.0013–0.0024 μm in the near-infrared ($R \approx 920$). A detailed atlas of the transmission spectrum with identifications of the main atomic and molecular absorption features is available (Supplementary Fig. 3). **b**, A comparison between the Earth's transmission (black) and reflection (blue) spectra. Both spectra have been degraded to a spectral resolution of 0.02 μm and normalized at the same flux value at around 1.2 μm . It is readily seen from the figure that the reflection spectrum shows increased Rayleigh reflectance in the blue. It is also noticeable how most of the molecular spectral bands are weaker, and some non-existent, in the reflection spectrum. In **a** and **b**, the noise (r.m.s.) of the spectra, which takes into account the corrections for the strongest local telluric features, is plotted point-per-point (in grey for black lines, in light blue for dark blue line) along with the spectra, although, for most spectral regions, the size of the error bars is comparable to the width of the line. The quality of the transmission data are measured in terms of signal-to-noise ratio, which goes from ~ 100 (at the deepest absorptions features and the blue optical wavelengths) up to ~ 400 (at the largest values of the relative fluxes).

¹Instituto de Astrofísica de Canarias, Vía Láctea s/n, E38205 La Laguna, Tenerife, Spain. ²Physics Department, University of Central Florida, PO Box 162385, Orlando, Florida 32816, USA.

Table 1 | Equivalent widths of the major molecular absorption features in Earth's spectra

Atmospheric species	Wavelength interval (μm)	Equivalent width, transmission (\AA)	Equivalent width, reflection (\AA)
O ₂ -a	0.6858–0.6952	17.0 \pm 0.4	13.5 \pm 1.0
O ₂ -b	0.7570–0.7706	55.0 \pm 0.3	47.8 \pm 1.0
H ₂ O-a	0.7133–0.7342	12.2 \pm 1.0	34.0 \pm 1.0
H ₂ O-b	0.8057–0.8400	21.2 \pm 1.0	50.8 \pm 5.0
H ₂ O-c	0.8884–0.9966	331.1 \pm 9.0	205.3 \pm 6.0
H ₂ O-d	1.0870–1.1755	381.0 \pm 9.0	160.71 \pm 10.0
H ₂ O-e	1.3000–1.5212	1,300.0 \pm 30.0	623.4 \pm 30.0
H ₂ O-f	1.7586–1.9824	1,111.0 \pm 30.0	350.0 \pm 80.0
O ₂ •O ₂ -a	0.5556–0.6200	71.1 \pm 4.0	\leq 50.0
O ₂ •O ₂ -b	1.0295–1.0872	69.0 \pm 2.0	<5.0
O ₂ O ₂ •O ₂ O ₂ •N ₂ -ab	1.2347–1.2853	178.9 \pm 9.0	24.2 \pm 3.0
CO ₂ -a	1.5629–1.5908	52.6 \pm 1.0	10.0 \pm 3.0
CO ₂ -b	1.5908–1.6214	54.8 \pm 1.0	12.0 \pm 3.0
CO ₂ -c	1.9906–2.0373	150.6 \pm 1.0	23.0 \pm 5.0
CO ₂ -d	2.0373–2.0789	127.6 \pm 1.0	<15.0
CH ₄ -a	1.6214–1.6750	58.0 \pm 1.0	<15.0
CH ₄ -bcd	2.1390–2.4000	>790	>280.0

Equivalent widths are measured with respect to the pseudo-continuum that is absorbed by much wider features, like Rayleigh scattering or extended water bands. The second column is indicative of the wavelength range over which the various features are integrated. In all cases, except for a few features in the optical, the equivalent widths are larger in the transmission spectrum than in the reflectance data. The indices -a to -f in the first column are used to compare with the filter sets defined in Supplementary Table 1.

In contrast, the Earth's reflection spectrum appears blue¹⁵ because the very same Rayleigh scattering effect expels the short wavelength radiation back to space. Because of the blue colour, when observed from an astronomical distance, the Earth is often referred to as the pale blue dot, but in transmission, the pale blue dot becomes the pale red dot.

Moreover, the transmission spectrum (Supplementary Fig. 3) presents strong absorption features produced by molecular oxygen and oxygen collision complexes, including collisions between O₂ and N₂, which are significantly more intense than in the reflection spectrum. Oxygen collision complexes are van der Waals molecules, also known as dimers^{16–18}, which can be used in combination with other molecular oxygen bands to derive an averaged atmospheric column density of N₂. This is important, because although N₂ is the major atmospheric component (78.08% by volume), it lacks any marked electronic transition. The strength of these bands in the transmission spectrum implies that atmospheric dimers may become a major subject of study for the interpretation of rocky exoplanet transmission spectra and their atmospheric characterization. The atmospheric spectral bands of O₃, O₂, H₂O, CO₂ and CH₄ are readily distinguishable in the transmission spectrum (Supplementary Fig. 3). Trace amounts of N₂O, OClO and NO₂ (a gas mainly produced by human activities) might also be present in our data, but their detection will need future detailed modelling efforts to fit the observations.

The presence of the Earth's ionosphere is also revealed in our transmission spectrum through the detection of relatively weak and narrow absorption lines corresponding to singly ionized calcium atoms (Ca II, Supplementary Fig. 3). Calcium is the sixth most abundant element on Earth. It is possible that other, more abundant^{19,20} ionospheric species, such as singly ionized magnesium (Mg II), could be detectable at shorter wavelengths that are not covered by our data. The neutral atomic resonance doublet of sodium (Na I) is embedded in a quite strong and broad absorption due to dimers, ozone and Rayleigh scattering, and only the core of the doublet is detected at 0.5898 μm .

In the coming years, space missions such as the James Webb Space Telescope will perhaps have the opportunity to perform transit spectroscopy of rocky exoplanets^{21,22}. The faint signal of the planet atmosphere will be mixed with the light of the parent star, and it is foreseen that many transits will have to be observed²³ before a good quality transmission spectrum of an exo-Earth can be obtained. Our empirical transmission spectrum suggests, however, that retrieving the major planetary signals might be easier than model calculations suggest. Observations of about 20–30 one-hour transits should yield the detection of the major spectral features in the transmission spectrum of an Earth-like planet around a low-mass M-type star in the solar neighbourhood. With this goal in mind, it is necessary to determine and quantify the observational requirements to detect each specific

molecule using the transmission spectrum presented here. It is also useful to compare the potential results from two exoplanet atmospheric characterization techniques: direct detection and transit spectroscopy.

Observations of the earthshine—the light reflected from the dark side of the Moon—are often obtained and studied as a proxy for direct extrasolar planet observations^{9,24–27}, mainly using chronographic or interferometric techniques^{28,29}. Here, we were able to carry out earthshine observations with the same instrumental set-up as that during our lunar eclipse observations (see Supplementary Information for details about our data acquisition and analysis). The data are displayed in Fig. 1b for comparison with the transmission spectrum.

The depth of the features in the reflection spectrum of the Earth can vary depending on (1) changes in the properties of the surface from which part of the light is being reflected, and (2) changes in the cloud coverage of the globe^{25,30}. However, these variations are typically small (\leq 6%) and they do not modify significantly the shape of the data. In the transmission spectrum, there is a negligible contribution from light reflecting from the Earth's surface, thus only the changes in cloudiness can affect the depth of the absorption features, and we expect the amplitude of the spectral variability to be at most of the same order as in the reflection spectrum.

In Table 1 are listed the major molecular features in the transmission and reflection spectra, together with their equivalent widths measured over the original data with a resolution of 0.0013–0.0024 μm . Even at very low signal-to-noise ratios, the major atmospheric components remain marginally detectable in the transmission spectrum, but not in the reflection spectrum (see Supplementary Information for a detailed analysis of confidence of detection of atmospheric features at different signal-to-noise levels). Thus, the transmission spectrum can provide much more information about the atmospheric composition of a rocky planet than the reflection spectrum can.

Received 30 December 2008; accepted 8 April 2009.

1. The Extrasolar Planets Encyclopaedia. (<http://exoplanet.eu>) (accessed 18 March 2009).
2. Seager, S. & Sasselov, D. D. Theoretical transmission spectra during extrasolar giant planet transits. *Astrophys. J.* **537**, 916–921 (2000).
3. Charbonneau, D., Brown, T. M., Noyes, R. W. & Gilliland, R. L. Detection of an extrasolar planet atmosphere. *Astrophys. J.* **568**, 377–384 (2002).
4. Tinetti, G. *et al.* Water vapour in the atmosphere of a transiting extrasolar planet. *Nature* **448**, 169–171 (2007).
5. Swain, M. R., Vasisht, G. & Tinetti, G. The presence of methane in the atmosphere of an extrasolar planet. *Nature* **452**, 329–331 (2008).
6. Mayor, M. *et al.* The HARPS search for southern extra-solar planets. XIII. A planetary system with 3 super-Earths (4.2, 6.9, and 9.2 M_E). *Astron. Astrophys.* **493**, 639–644 (2009).

7. Borde, P., Rouan, D. & Leger, A. Exoplanet detection capability of the COROT space mission. *Adv. Space Res.* **405**, 1137–1144 (2003).
8. Basri, G., Borucki, W. J. & Koch, D. The Kepler Mission: A wide-field transit search for terrestrial planets. *N. Astron. Rev.* **49**, 478–485 (2005).
9. Montañés-Rodríguez, P., Palle, E., Goode, P. R., Hickey, J. & Koonin, S. E. Globally integrated measurements of the Earth's visible spectral albedos. *Astrophys. J.* **629**, 1175–1182 (2005).
10. Ehrenreich, D., Tinetti, G., Lecavelier Des Etangs, A., Vidal-Madjar, A. & Selsis, F. The transmission spectrum of Earth-size transiting planets. *Astron. Astrophys.* **448**, 379–393 (2006).
11. Miller-Ricci, E., Seager, S. & Sasselov, D. The atmospheric signatures of super-earths: How to distinguish between hydrogen-rich and hydrogen-poor atmospheres. *Astrophys. J.* **690**, 1056–1067 (2009).
12. Slipher, V. M. On the spectrum of the eclipsed Moon. *Astron. Nachr.* **199**, 103 (1914).
13. Moore, J. H. & Brigham, L. A. The spectrum of the eclipsed Moon. *Publ. Astron. Soc. Pacif.* **39**, 223–226 (1927).
14. Shane, C. D. Photographs of the lunar eclipse of June. *Publ. Astron. Soc. Pacif.* **39**, 226–228 (1927).
15. Sagan, C., Thompson, W. R., Carlson, R., Gurnett, D. & Hord, C. A search for life on Earth from the Galileo spacecraft. *Nature* **365**, 715–718 (1993).
16. Calo, J. & Narcisi, R. Van der Waals molecules — possible roles in the atmosphere. *Geophys. Res. Lett.* **7**, 289–292 (1980).
17. Klemperer, W. & Vaida, V. Molecular complexes in close and far away. *Proc. Natl Acad. Sci. USA* **103**, 10584–10588 (2006).
18. Solomon, S., Portmann, R. W., Sanders, R. W. & Daniel, J. S. Absorption of solar radiation by water vapor, oxygen, and related collision pairs in the Earth's atmosphere. *J. Geophys. Res.* **103** (D4), 3847–3858 (1998).
19. Zbinden, P. A., Hidalgo, M. A., Eberhardt, P. & Geiss, J. Mass spectrometer measurements of the positive ion composition in the D- and E-regions of the ionosphere. *Planet. Space Sci.* **23**, 1621–1642 (1975).
20. Kopp, E. On the abundance of metal ions in the lower ionosphere. *J. Geophys. Res.* **102** (A5), 9667–9674 (1997).
21. Gardner, J. P. *et al.* The James Webb Space Telescope. *Space Sci. Rev.* **123**, 485–606 (2006).
22. Charbonneau, D. & Deming, D. The dynamics-based approach to studying terrestrial exoplanets. Preprint at (<http://arXiv.org/abs/0706.1047>) (2007).
23. Kaltenegger, L. & Traub, W. A. Transits of Earth-like planets. *Astrophys. J.* (in the press); preprint at (<http://arXiv.org/abs/0903.3371v2>) (2009).
24. Woolf, N. J., Smith, P. S., Traub, W. A. & Jucks, K. W. The spectrum of earthshine: A pale blue dot observed from the ground. *Astrophys. J.* **574**, 430–433 (2002).
25. Montañés-Rodríguez, P. P., Palle, E. & Goode, P. R. Vegetation signature in the observed globally-integrated spectrum of Earth: modeling the red edge strength using simultaneous cloud data and applications for extrasolar planets. *Astrophys. J.* **651**, 544–552 (2006).
26. Turnbull, M. C. *et al.* Spectrum of a habitable world: Earthshine in the near-infrared. *Astrophys. J.* **644**, 551–559 (2006).
27. Palle, E., Goode, P. R., Montañés-Rodríguez, R. & Koonin, S. E. Changes in the Earth's reflectance over the past two decades. *Science* **304**, 1299–1301 (2004).
28. Cash, W. Detection of Earth-like planets around nearby stars using a petal-shaped occulter. *Nature* **442**, 51–53 (2006).
29. Lindensmith, C. Terrestrial planet finder: technology development plans. Optical, infrared, and millimeter space telescopes. *Proc. SPIE* **5487**, 1226–1233 (2004).
30. Palle, E., Ford, E. B., Seager, S., Montañés-Rodríguez, P. & Vázquez, M. Identifying the rotation rate and the presence of dynamic weather on extrasolar Earth-like planets from photometric observations. *Astrophys. J.* **676**, 1319–1329 (2008).

Supplementary Information is linked to the online version of the paper at www.nature.com/nature.

Acknowledgements We thank F. Grundahl and J. Fynbo for allowing us access to their awarded time at the Nordic Optical Telescope, thus making this work possible. We are also grateful to V. J. S. Béjar, E. Guinan, S. Seager, B. Portmann, A. Garcia-Muñoz and Y. Pavlenko for discussions. Support for this project was provided by the Spanish Ministry of Science via the Ramon y Cajal fellowship (E.P.) and project AYA2007-67458. This work was based on observations made with the WHT (operated by the Isaac Newton Group) and the NOT (operated by Denmark, Finland, Iceland, Norway and Sweden), both on the island of La Palma in the Spanish Observatorio del Roque de los Muchachos of the Instituto de Astrofísica de Canarias.

Author Information Reprints and permissions information is available at www.nature.com/reprints. Correspondence and requests for materials should be addressed to E.P. (epalle@iac.es).